Springer

Journal of Mechanical Science and Technology 22 (2008) 1952~1958

Journal of
Mechanical
Science and
Technology

www.springerlink.com/content/1738-494x
DOI 10.1007/s12206-008-0738-5

Heat/Mass transfer measurement on concave surface in rotating jet impingement †

Sung Kook Hong, Dong Hyun Lee and Hyung Hee Cho*

Department of Mechanical Engineering, Yonsei University, Seoul 120-749 Korea

(Manuscript Received April 16, 2008; Revised June 23, 2008; Accepted July 23, 2008)

Abstract

The objective of this paper is to investigate the heat/mass transfer characteristics on a concave surface for rotating impinging jets. The jet with Reynolds number of 5,000 is applied to the concave surface and the flat surface, respectively. The rotating experiments have been carried out at the rotating speed of 560RPM which is corresponding to Ro number of 0.075. The two jet orientation (front and trailing orientation) are considered. Detailed heat/mass transfer coefficients on the target plate were measured using a naphthalene sublimation method. The result indicates that the rotation leads to change in local heat/mass transfer distributions and the slight increase in the Sh level. The front orientation induces asymmetric Sh distributions, whereas the trailing orientation shows the shifted heat/mass transfer feature due to rotation-induced flow behavior. The crossflow effect on heat/mass transfer is also observed as the streamwise direction increases. Compared to flat surface, the heat/mass transfer on the concave surface is enhanced with increasing the spanwise direction due to the curvature effect, providing the higher averaged Sh value. It is proved that the difference of surface geometry affects somewhat the local and averaged heat/mass transfer regardless of rotation condition.

Keywords: Impinging jet; Heat/mass transfer; Naphthalene sublimation method; Rotation; Concave surface

1. Introduction

Heat transfer under impinging jet is generally superior to that achieved with typical convective heat transfer methods. The impingement cooling jet has an advantage that it is easy to adjust the location of interest and remove a large amount of heat effectively. Owing to the benefits, the impinging jets are used widely in many industrial systems, including high temperature gas turbines, and high density electrical and electronic equipment. Therefore, a lot of studies related to impinging jet have been carried out, and Martin [1] and Viskanta [2] reviewed extensively the previous studies of impingement heat transfer.

However, there are still few studies on the concave surface while a lot of studies of impinging jet are related to the flat surface. Gau and Jung [3], and Yang et al. [4] investigated the flow and heat transfer characteristics depending on various parameters such as jet Reynolds number, slot to plate spacing and slot width. They showed that heat transfer rates for impingement on the concave surface are more enhanced than those on the flat plate results due to the curvature effect. Cornaro et al. [5] measured the local flow behavior using flow visualizations and showed that the flow over a concave surface is more unsteady than that on convex surface. However, these studies are confined to the slot jet or single jet only under stationary condition. Regarding the rotating impinging jet, few studies have been reported. Epstein et al. [6] investigated the heat transfer characteristics of array jet cooling on concave surface. They showed that the rotation reduces the heat transfer and changes the local heat transfer distributions. Mattern et al. [7]

† This paper was presented at the 9th Asian International Conference on Fluid Machinery (AICFM9), Jeju, Korea, October 16-19, 2007.

*Corresponding author. Tel.: +82 2 2123 2828, Fax.: +82 2 312 2159
E-mail address: hhcho@yonsei.ac.kr

reported the local heat/mass transfer distributions on the curved impinging plate with regard to various parameters such as hole-to-hole spacing, hole-to-plate spacing, and jet orientation. Iacovides et al. [8] researched the impinging jet under the ultimate rotation condition with Ro = 0.18 and suggested the Nusselt number on the impinging surface. They reported that all secondary peaks and some of the primary peaks in array jets disappear due to strong rotation effect.

As mentioned, there is limited information of the local heat transfer on the concave surface with rotation. The detailed heat transfer coefficients are required for the application such as impinging jet cooling in the leading edge region of turbine blade with curved surface. Therefore, in the present study, the local heat/mass transfer characteristics have been investigated for rotating array jet cooling on the concave surface and the results are compared with those of flat surface to evaluate the influence of surface geometry. A naphthalene sublimation method is used to measure local heat/mass transfer coefficients on the target plate.

2. Experimental apparatus and conditions

2.1 Experimental apparatus

Fig. 1 shows the rotating apparatus that composes of a rotating plate with a diameter of 1 m, blower, heat exchanger, and test duct designed for the array jet cooling. A test duct, multimeter and Bluetooth device are installed on the rotating plate. By Bluetooth device, the temperature measured in the test duct is transferred into an external computer wirelessly in real time. The speed of the rotating plate is controlled by an inverter and a tachometer. Air is supplied by the inverter-controlled blower (7.5 kW) and the flow rate is measured using an orifice flowmeter. The temperature of air is maintained to be constant throughout the heat exchanger using a constant-temperature reservoir.

To evaluate the curvature effect on heat transfer characteristics, the concave duct and the flat duct are considered as shown in Fig. 2. The diameter (d) of injection hole is 10 mm. For the concave duct, the diameter of semicircle (D_C) is 60 mm and consequently the curvature parameter (D_C/d) is to be 6. The hydro-diameter of concave duct (D_h) is 36.66 mm. Meanwhile, for the flat duct, the width (W) is 50 mm and the height (H) is 30 mm, providing the hydro-

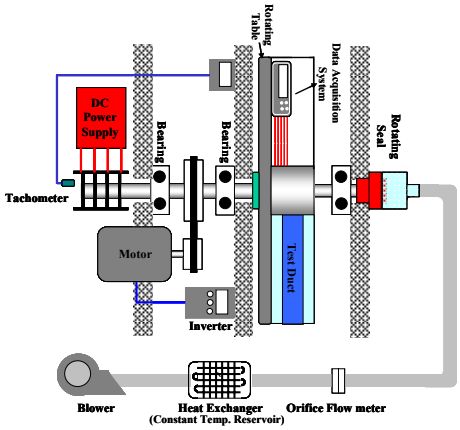

Fig. 1. Schematic view of experimental facility.

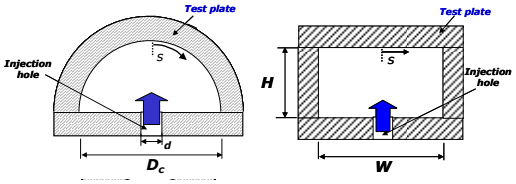

(a) Concave duct (b) Flat duct

Fig. 2. Cross-sectional geometry of test duct.

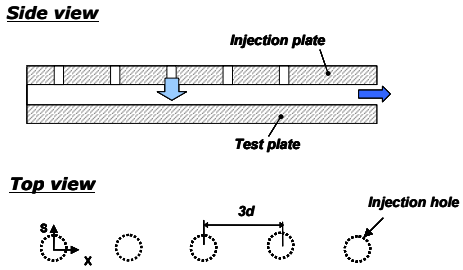

Fig. 3. Schematic view of test duct.

diameter (D_h) to be 37.5 mm. The mean rotating radius of the test duct is equal to 320 mm.

As shown in Fig. 3, the five injection holes are applied to the injection plate. After jet impingement, the spent air is discharged through one-sided exit into the outside. Hole-to-plate spacing ratio (H/d) is 3.0 and hole-to-hole spacing ratio (P_{hole}/d) is 3.0 for the streamwise direction. To measure the local heat/mass transfer coefficients on the target plate, a naphthalene-coated test plate is installed at the test duct.

2.2 Operating conditions

The rotating experiments have been carried out at

the fixed rotating speed of 560 RPM, corresponding to Ro number of 0.075. The jet Reynolds number based on the injection hole diameter is 5,000. To examine the effect of the jet orientation, two jet orientations are considered in the present study. Depending on the jet orientation to the rotation axis, the injected jet flow is differently influenced by the Coriolis force. When the jet flow is parallel to rotation axis, the injected jet is not directly affected by the Coriolis force. However, when the jet flow is orthogonal to the rotation axis, the Coriolis force acts on the injected jet flow toward the specific direction which is the inward direction with respect to the origin of rotation axis (in the present experiment). The each orientation is referred to as the front and trailing orientation, respectively.

2.3 Data reduction

To obtain local mass transfer coefficients, the variation of the naphthalene surface is measured on the measurement tables before and after each test run. The details of measuring system are described by Goldstein and Cho [9]. The local mass transfer coefficient is defined as:

$$h_m = \frac{\dot{m}}{\rho_{v,w} - \rho_{v,\infty}} = \frac{\rho_s (dy/d\tau)}{\rho_{v,w}} \quad (1)$$

Since the incoming flow contains no naphthalene, $\rho_{v,\infty}$ is zero in the present study. The Sherwood number can be expressed as:

$$\mathrm{Sh} = h_m d / D_{naph} \quad (2)$$

D_{naph} is the diffusion coefficient of naphthalene vapor in air and the properties of naphthalene suggested by Goldstein and Cho [9] are used in the present study. The mass transfer coefficients can be converted to the heat transfer coefficients using the heat and mass transfer analogy by Eckert [10]. Uncertainty of the Sherwood numbers using the method reported by Abernethy et al. [11] is within ±8.7% in the entire operating range of the measurement, based on a 95% confidence interval. This uncertainty is mainly attributed to the uncertainty of the properties of naphthalene, such as the naphthalene saturated vapor density (6.9%) and diffusion coefficient of naphthalene vapor in air (5.1%). The other uncertainties are 1.1% and 7.0% for density of solid naphthalene and mass transfer coefficient, respectively.

3. Result and discussion

3.1 Heat/mass transfer characteristics

Fig. 4 shows the contour plots of Sh on the concave surface where the white circle indicates the position of projected injection hole. For the stationary case, the high heat/mass transfer region is observed around the stagnation region due to the thin hydrodynamic and thermal boundary layers by jet impingement [1]. Since the crossflow is generated by the spent air from impinging jets in a confined duct, the crossflow effect becomes strong with increasing x/d. Therefore, the position of stagnation point moves downstream and its value increases due to the interaction between impinging jet and crossflow reported by Rhee et al. [12].

When the test duct is rotating at the front orientation (Fig. 4(b)), the asymmetry Sh pattern is observed. This is possibly due to the rotation-induced flow behavior. After the jet impingement on the target plate, the turning jet flow develops along all directions from the stagnation point. Since the direction of developing

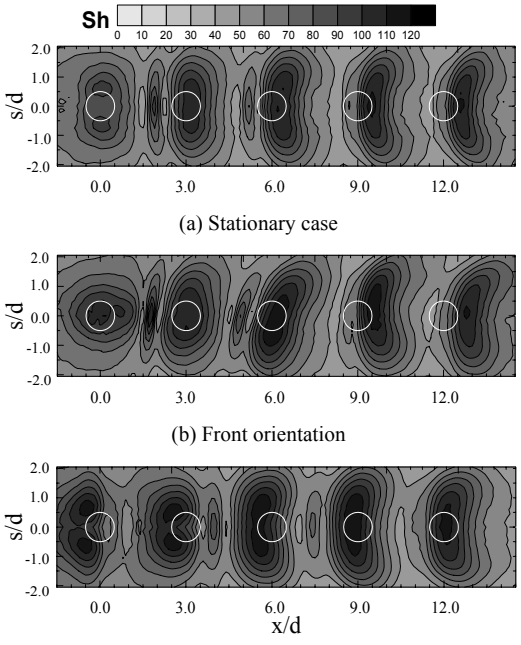

(a) Stationary case

(b) Front orientation

(c) Trailing orientation

Fig. 4. Contour plots of Sh on concave surface at various rotating conditions.

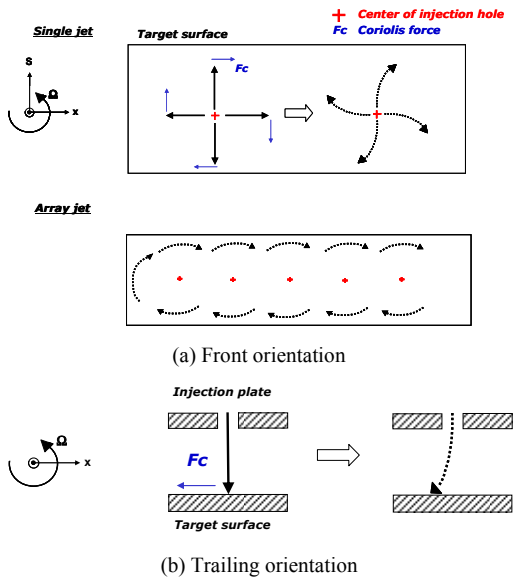

Fig. 5. Expected flow pattern at different jet orientation.

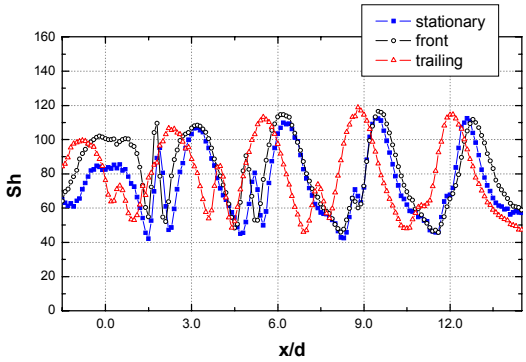

Fig. 6. Local plot of Sh on concave surface along s/d = 0.0 at various rotating conditions.

flow is orthogonal to the rotation axis, the developing flow is affected by the Coriolis force. Therefore, each developing flow from the stagnation point is somewhat deflected in the clockwise direction while the test duct rotates in the counterclockwise direction as shown in Fig. 5(a). For the array jet, the similar deflected flow behavior occurs in the confined duct and consequently Sh distributions of top region (s/d > 0.0) shifted to right side compared to those of bottom region (s/d < 0.0). Further, the Sh level is enhanced due to the increase in flow mixing by the rotation. For trailing case (Fig. 4(c)), the stagnation region moves upstream and the shifted Sh distributions are formed compared to other cases. It is attributed to the jet deflection effect by the Coriolis force as described in

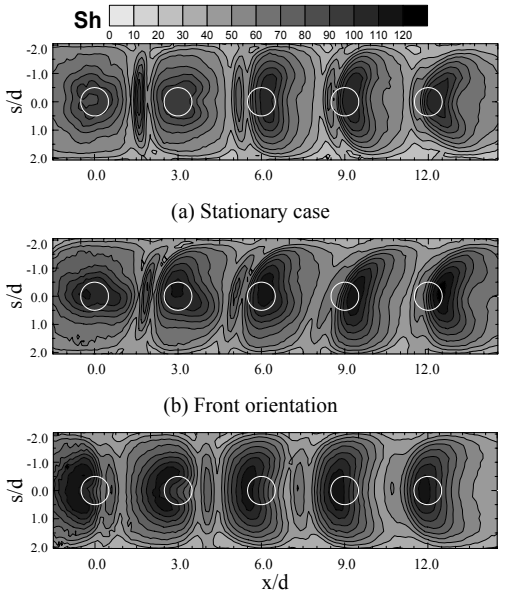

Fig. 7. Contour plots of Sh on flat surface at various rotating conditions.

Fig. 5(b). However, the shifted feature decreases gradually with increasing x/d because the crossflow effect becomes strong.

In both stationary and trailing case, the separated peaks are observed apparently around the first injection hole region (x/d ≅ 0.0) which is not affected by crossflow. It is possibly because the curvature effect leads to increase the turbulence intensity of accelerated jet flow at stagnation region. Meanwhile, for front orientation, this feature is not shown due to strong flow mixing induced by rotation.

Fig. 6 shows local Sh distributions along s/d = 0.0 at the various rotating cases. The Sh features by rotation are observed such as the increased Sh and the shifted Sh at the stagnation region compared to that of stationary case. Meanwhile, as x/d increases, the first peak value rises and the secondary peak by adjacent jet interaction weakens due to the accumulated crossflow rate.

3.2 Comparison of concave surface with flat surface

To investigate the curvature effect, the experiments on flat surface have been conducted. Fig. 7 shows the contour plots of Sh on the flat surface. The overall Sh distributions on flat surface are similar to those on concave surface (Fig. 4) and the Sh features by rota-

tion are also observed; the asymmetric Sh for the front orientation and the shifted Sh for the trailing orientation. However, some discrepancy caused by surface geometry is observed. To show more clearly, Fig. 8 compares local Sh on the concave surface with that on the flat surface at the region of x/d = 0.0 which is not affected by crossflow.

In stationary case (Fig. 8(a)), the Sh on the concave surface becomes higher than that on the flat surface as the spanwise direction (s/d) increases from stagnation point (s/d = 0.0). It is attributed to the curvature effect which promotes the flow mixing and then enhances the heat/mass transfer [3]. Moreover, the apparent peaks are observed approximately 0.5d apart from stagnation point. It is possibly because the curvature effect strengthens the turbulence intensity in the accelerated flow at the stagnation region.

For the front orientation (Fig. 8(b)), the difference by surface geometry becomes relatively small, showing slight Sh increase near s/d = ±2.0. It is because the rotation with front orientation increases the flow mixing significantly regardless of the surface geometry and then the additional increase in flow mixing by the curvature effect is not great. On the contrary, for the trailing orientation (Fig. 8(c)), the rotation makes the impinging jet shift upstream and does not significantly affect the flow mixing along the spanwise direction. Therefore, the Sh enhancement due to curva

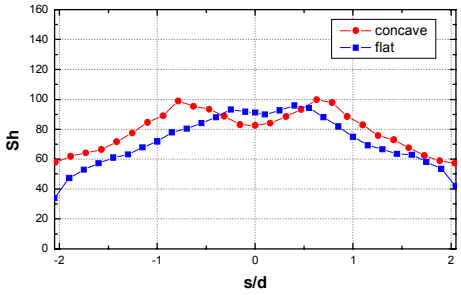

(a) Stationary case

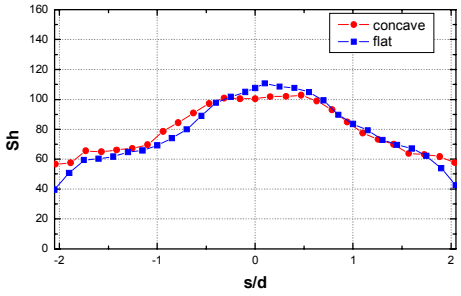

(b) Front orientation

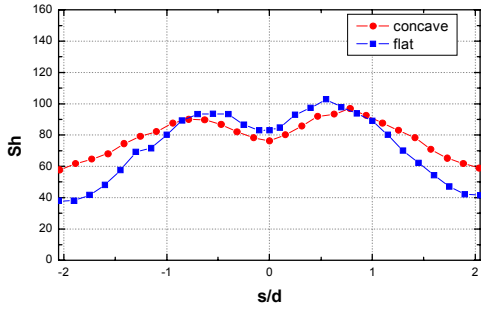

(c) Trailing orientation

Fig. 8. Local plots of Sh on along x/d = 0.0 at different surface geometry.

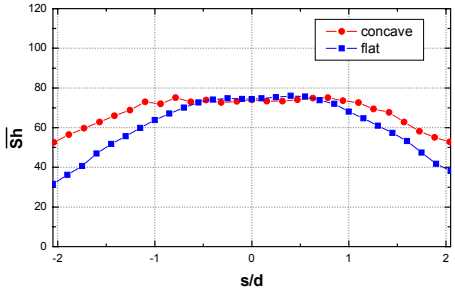

(a) Stationary case

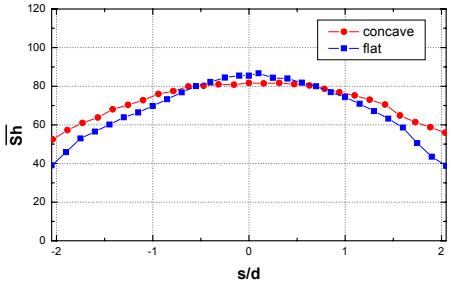

(b) Front orientation

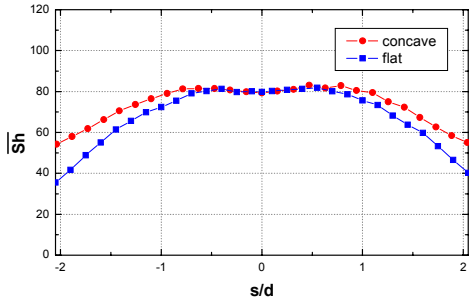

(c) Trailing orientation

Fig. 9. Spanwise averaged Sh at different surface geometry.

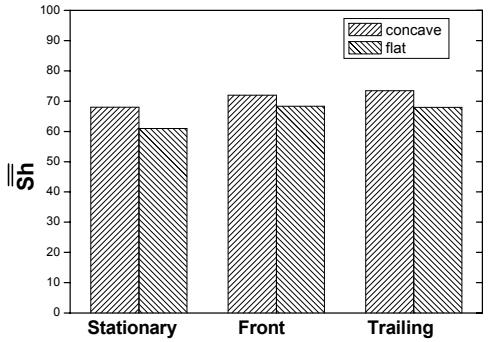

Fig. 10. Averaged Sh for the tested cases.

ture effect becomes great with increasing s/d.

Fig. 9 shows the spanwise averaged Sh distributions at the various rotation conditions. This value is calculated by averaging the local data in the range of $-1.5 \leq x/d \leq 14.5$. At the stagnation region, Sh values on the concave surface are similar to those on the flat surface. However, the spanwise averaged Sh value becomes higher than that on the flat surface with increasing s/d. These features are observed regardless of the rotation condition.

Fig. 10 presents the averaged Sh value which is calculated by averaging the local data in the range of $-1.5 \leq x/d \leq 14.5$ and $-2.05 \leq s/d \leq 2.05$. The averaged Sh value in the concave surface is higher than that in the flat surface due to the curvature effect. Therefore, it is proved that the difference of surface geometry affects somewhat the averaged heat transfer value regardless of rotation condition. Meanwhile, the rotation yields the slight augmentation in averaged Sh value. It is mainly that the rotation increases the flow mixing in the confined duct with small H/d.

4. Conclusions

In the present study, the heat/mass transfer characteristics on the concave surface are investigated for the impinging jet cooling with rotation and compared with those of flat surface. The results are summarized as follows:

Within the confined duct, the heat/mass transfer characteristics are changed by the rotation and the crossflow effect. The front (parallel) orientation leads to asymmetric Sh distributions, whereas the trailing (orthogonal) orientation shows the shifted Sh distribution due to rotation-induced flow behavior. The heat/mass transfer is slightly enhanced because of increase in flow mixing by rotation. The crossflow effect on heat/mass transfer is also observed with increasing the streamwise direction.

Compared to flat surface, the heat/mass transfer on the concave surface is enhanced with increasing the spanwise direction due to the curvature effect, providing the higher averaged Sh value. Therefore, it is proved that the difference of surface geometry affects somewhat the local and averaged heat/mass transfer regardless of rotation condition.

Acknowledgments

The authors wish to acknowledge support for this study partially by the Electric Power Industry Technology and Planning.

Nomenclature

dy:	:	Local sublimation depth of naphthalene
d	:	Injection hole diameter
D_c	:	Diameter of semicircle in concave test duct
D_h	:	Hydraulic diameter of test duct
D_{naph}	:	Mass diffusion coefficient of naphthalene vapor in air
H	:	Gap distance between injection hole and target surface
h_m	:	Local mass transfer coefficient , Eq. (1)
$\dot{m}$	:	Local naphthalene mass transfer per unit area and time
P_{hole}	:	Pitch of injection holes at injection plate
Re_d	:	Reynolds number based on hole diameter and the average velocity in the hole
Ro	:	Rotation number, $\Omega d/V_i$
Sh	:	Sherwood number based on the hole diameter
$\overline{Sh}$	:	Spanwise averaged Sherwood number
$\overline{\overline{Sh}}$	:	Overall averaged Sherwood number
V_i	:	Mean velocity of impinging jet
x, s	:	Distance from the center of injection hole
Ω	:	Rotation velocity

Greek symbols

ρ_s	:	Density of solid naphthalene
$\rho_{v,w}$	:	Naphthalene vapor density on the surface
$\rho_{v,\infty}$	:	Naphthalene vapor density of the injected jet
$d\tau$	:	Test duration

References

[1] H. Martin, Heat and mass transfer between impinging gas jets and solid surfaces, *Adv. Heat Mass Transfer*, 13 (1977) 1-60.

[2] Viskanta, Heat transfer to impinging isothermal gas and flame jets, *Experimental Thermal and Fluid Science*, 6 (1993) 111-134.

[3] C. Gau and C. M. Chung, Surface Curvature Effect on Slot-Air-Jet Impingement Cooling Flow and Heat Transfer Process, *Journal of Heat Transfer*, 113 (1991) 858-864.

[4] G. Yang, M. Choi and J. S. Lee, An experimental study of slot jet impingement cooling on concave surface: effects of nozzle configuration and curvature, *International Journal of Heat and Mass Transfer*, 42 (1999) 2199-2209.

[5] C, Cornaro, A. S. Fleischer and R. J. Goldstein, Flow visualization of a round jet impinging on cylindrical surfaces, *Experimental Thermal and Fluid Science*, 20 (1999) 66-78.

[6] A. H. Epstein, J. L. Kerrebrock, J. J. Koo and U. Z. Preiser, Rotational Effects on Impingement Cooling, (1985) *GTL Report* No. 184.

[7] Ch. Mattern and D. K. Hennecke, The influence of rotation on impingement cooling, (1996) *ASME paper* No. 96-GT-161.

[8] H. Iacovides, D. Kounadis, B. E. Launder, J. Li and Z. Xu, Experimental Study of the Flow and Thermal Development of a Row of Cooling Jets Impinging on a Rotating Concave Surface, *Journal of Turbomachinery*, 127 (2005) 222-229.

[9] R. J. Goldstein and H. H. Cho, A Review of Mass Transfer Measurement Using Naphthalene Sublimation, *Experimental Thermal and Fluid Science*, 10 (1995) 416-434.

[10] E. R. G. Eckert, Analogies to Heat Transfer Processes, in Measurements in Heat Transfer, ed. E. R. G. Eckert and R. J. Goldstein, *Hemisphere Pub.*, New York. (1976) 397-423.

[11] R. B. Abernethy, R. P. Benedict and R. B. Dowdell, Measurement Uncertainty, *Journal of Fluid Engineering*, 107 (1985) 161-164.

[12] D. H. Rhee, P. H. Yoon and H. H. Cho, Local Heat/Mass Transfer and Flow Characteristics of Array Impinging Jets with Effusion Holes Ejecting Spent Air, *International Journal of Heat and Mass Transfer*, 46 (2003) 1049-1061.